Life Sciences 239 (2019) 116880

Contents lists available at ScienceDirect

Life Sciences

journal homepage: www.elsevier.com/locate/lifescie

Rolipram optimizes therapeutic effect of bevacizumab by enhancing proapoptotic, antiproliferative signals in a glioblastoma heterotopic model

Sara Ramezani[a,b,c], Nasim Vousooghi[d,e,f,*], Fatemeh Ramezani Kapourchali[g], Shahrokh Yousefzadeh-Chabok[a,b,**], Zoheir Reihanian[h], Ali Mohammad Alizadeh[i], Saeed Khodayari[i], Hamid Khodayari[i]

[a] Neuroscience Research Center, School of Medicine, Guilan University of Medical Sciences, Rasht, Iran
[b] Guilan Road Trauma Research Center, School of Medicine, Guilan University of Medical Sciences, Rasht, Iran
[c] Cellular and Molecular Research Center, Iran University of Medical Sciences, Tehran, Iran
[d] Department of Neuroscience and Addiction Studies, School of Advanced Technologies in Medicine, Tehran University of Medical Sciences, Tehran, Iran
[e] Research Center for Cognitive and Behavioral Sciences, Tehran University of Medical Sciences, Tehran, Iran
[f] Iranian National Center for Addiction Studies (INCAS), Tehran University of Medical Sciences, Tehran, Iran
[g] Department of Inflammation and Immunity, Lerner Research Institute, Cleveland Clinic, Cleveland, OH, 44195, USA
[h] Neurosurgery Department, Guilan University of Medical Sciences, Guilan, Iran
[i] Cancer Research Center, Tehran University of Medical Sciences, Tehran, Iran

ARTICLE INFO

Keywords:
Antiangiogenesis therapy
Phosphodiesterase IV
Hypoxia
Apoptosis
AKT signal
Combination therapy

ABSTRACT

The unstable response to bevacizumab is a big dilemma in the antiangiogenic therapy of high-grade glioma that appears to be linked to an increase in the post-treatment intratumor levels of hypoxia-inducible factor 1 α (HIF1α) and active AKT. Particularly, a selective phosphodiesterase IV (PDE4) inhibitor, rolipram is capable of inhibiting HIF1α and AKT in cancer cells. Here, the effect of bevacizumab alone and in presence of rolipram on therapeutic efficacy, intratumor hypoxia levels, angiogenesis, apoptosis and proliferation mechanisms were evaluated. BALB/c mice bearing C6 glioma were received bevacizumab and rolipram either alone or combined for 30 days (n = 11/group). At the last day of treatments, apoptosis, proliferation and microvessel density, in xenografts (3/group) were detected by TUNEL staining, Ki67 and CD31 markers, respectively. Relative expression of target proteins was measured using western blotting. Bevacizumab initially hindered the tumor progression but its antitumor effect was weakened later despite the vascular regression and apoptosis induction. Unpredictably, bevacizumab-treated tumors exhibited the highest cell proliferation coupled with PDE4A, HIF1α and AKT upregulation and p53 downregulation and reversed by co-treatment with rolipram. Unlike a similar antivascular pattern to bevacizumab, rolipram consistently led to a more tumor growth suppression and proapoptotic effect versus bevacizumab. Co-treatment maximally hampered the tumor progression and elongated survival along with the major vascular regression, hypoxia, apoptosis induction, p53 and caspase activities. In conclusion, superior and persistent therapeutic efficacy of co-treatment provides a new insight into anti-angiogenic therapy of malignant gliomas, suggesting to be a potential substitute in selected patients.

1. Introduction

Apoptosis impairment and inordinate angiogenesis are the hallmarks of glioblastoma multiforme (GBM) [1] and are associated with tumor malignancy and poor prognosis [2,3]. Particularly, in a hypoxia-dependent angiogenesis manner, hypoxia-inducible factor 1 α (HIF1α) induces the vascular endothelial growth factor A ($VEGF_A$) transcription and secretion by GBM cells (GCs) on the endothelial cells (ECs) in a paracrine manner, developing neovascularization [4,5]. However, the role of HIF1α in apoptosis process is complex. HIF1α appears to have cell type-dependent pro- and antiapoptotic functions. Evidence has been highlighted that HIF1α may inhibit apoptosis in GBM [6].

Today, bevacizumab, a human recombinant monoclonal antibody, antagonizes $VEGF_A$ and routinely prescribed as an anti-angiogenesis

* Corresponding author. Department of Neuroscience and Addiction Studies, School of Advanced Technologies in Medicine, Tehran University of Medical Sciences, Tehran, Iran.
** Corresponding author. Neuroscience Research Center, School of Medicine, Guilan University of Medical Sciences, Rasht, Iran.
E-mail addresses: n-vousooghi@tums.ac.ir (N. Vousooghi), yousefzadeh@gums.ac.ir (S. Yousefzadeh-Chabok).

https://doi.org/10.1016/j.lfs.2019.116880
Received 17 June 2019; Received in revised form 18 August 2019; Accepted 15 September 2019
Available online 31 October 2019

agent for recurrent GBM patients in the clinic [7]. Based on the clinical data, bevacizumab brings about an early therapeutic efficacy [8–10] but tumor relapse inevitably emerges at long last [11,12]. Several scholars have sought to understand the refractoriness patterns of bevacizumab-treated tumors. According to prior findings, bevacizumab resistance mechanisms may be mediated through either a compensatory overactivation of some serine threonine kinases like AKT that may be triggered by binding some growth factors and their receptors in the absence of $VEGF_A$ [13,14] directly blocked by bevacizumab [14]or the hypoxia induction and an elevation of HIF1α levels [15–17] due to the vessel pruning caused by bevacizumab [16,18]. Thus, the serious efforts are required to identify a proper alternative therapeutic approach targeting GBM angiogenesis with no compensatory activation of alleged tumor recurrence mediators stimulated by bevacizumab, probably providing the more potent clinical benefits.

Recently, it has been revealed that phosphodiesterase IV (PDE4) contributes in the pathological angiogenesis [19,20] and tumorigenesis [21] of cancer. A piece of evidence uncovered a crosstalk between PDE4A and HIF1α in cancer cells to stimulate the tumor progression and angiogenesis that can be abrogated by a selective PDE4 inhibitor named rolipram [19]. A prior study on GCs also indicated that rolipram can attenuate the intracellular activity/phosphorylation of AKT, leading to the tumor cell apoptosis [22]. Hereby, it is supposed that the rolipram may beneficent for the enhancement of tumor response to bevacizumab in a combination therapeutic approach through targeting active AKT and HIF1α.

Although the anti-tumor action of bevacizumab [23] and rolipram [22,24–27] on the GBM reported in the past, the role of HIF1α in this regard has not been well elucidated, yet. Furthermore, there is an ambiguity based on whether bevacizumab in presence of rolipram may be more efficacious as compared to bevacizumab monotherapy in GBM heterotopic animal models and what the possible underlying mechanism(s) is. Biologically, the role of PDE4A, HIF1α, p53 and AKT signals in the development of this possible superiorities are unclear. Hereupon, it was of interest to clarify these indeterminacies.

2. Materials & methods cell culture and heterotopic glioma modeling

C6 glioma cells were expanded by three subcultures, as previously described [23]. The models were constructed through a subcutaneous injection of distinct suspensions comprising 3×10^6 C6 cells and 100 μl serum-free cell culture media into the right flank of 44 female 6–8 weeks old BALB/c mice having a bodyweight average about 18 ± 2 gr. The animals were cared in the appropriate home cages under a suitable condition for living. All processes were accomplished according to the National Institutes of Health Guide for the Care and Use of Laboratory Animals (NIH publication No. 85–23, revised 1985). Experimental protocols were approved by the Research and Ethics Committee of Guilan University of Medical Sciences.

3. Therapeutic schedule of tumor-bearing mice

Treatments were initiated after eighteen days of cell inoculation when tumor volume reached about 200–250 mm^3. At the start (on day 0), tumor-bearing mice were randomly assigned to four distinct experimental groups (n = 11/group). The animals were treated with clinical low dose of bevacizumab [28] (Avastin, Roche; intraperitoneally, 5 mg/kg, q2d × 11) or rolipram (Sigma-Aldrich; orally, 5 mg/kg/day), or bevacizumab plus rolipram, or bovine serum albumin (BSA, Sigma-Aldrich) as the control for 31 days, including day 0. To determine a tolerable and advantageous dosage of rolipram, a pilot study was done. On day 49th after cell implantation, treatments were finished and the mice (n = 3/group) were haphazardly set aside to be sacrificed. Afterward, tumors were immediately aspirated and protected under a proper condition to be evaluated in terms of subsequent molecular and histopathological changes after treatment.

4. Macroscopic and clinical measurements

Bodyweight fluctuation, tumor volume and growth inhibition in various groups using a set of formula were calculated as previously described [23]. The body weight and tumor size were measured once every 2 and 5 days, respectively. In order to determine survival time, the mice survivance were continuously monitored. Then, the number of days since the beginning of treatment until the mice's death for ethic limitations were counted enumerated. Lifespan percentage was computed as previously declared [23].

5. Tissue staining and microscopic analysis

First of all, formalin-fixed samples were processed and embedded in paraffin. Then, the slices with a thickness of 5 μm were provided from samples. Hematoxylin and eosin (H&E) staining was performed on the slices to the cellular density be measured. After the final step of staining, dehydrated slices were prepared to be observed under a microscope. Immunohistochemistry technique was started primarily by deparaffinization and rehydration of paraffin-embedded tissue sections followed by the antigen retrieval, heating, endogenous peroxidase blocking, and washing procedures were done, respectively. Then, to assess the cell proliferation and microvessel density, tissue sections were separately stained with primary antibodies against either Ki67 or CD31, respectively. Next staining steps were stated in the past [23]. After hematoxylin counterstaining and dehydration process, the slices were placed under a microscope. To estimate cell proliferation and vascular density, the number of cells stained with target markers of each filed were normalized to total hematoxylin-stained cells of the same field. To detect apoptotic cells, terminal deoxynucleotidyl transferase dUTP nick end labeling (TUNEL) staining was carried out according to the manufacturer's instructions (In Situ Cell Death Detection Kit, Fluorescein—Roche Applied Science; Switzerland). Before viewing the slices under a microscope, they were counterstained with propidium iodide (PI) to access to total nuclei per field of the section. Normalized mean value of cell apoptosis was acquired as previously described [23]. All slices were magnified by an inverted microscope (Olympus I×71) in three to four fields per section from individual xenografts and labeled cells semi-quantified using Image J software.

6. Western blot analysis

Tissue samples were lysed and the proteins extracted. After the quantification of protein concentration, successive stages of this technique accurately were conducted as previously described [23]. Applied antibodies in this study consist of total and phospho-AKT (Ser 473), p53, CA9 (as a hypoxia marker), HIF1α, PDE4A, cleaved-caspase3 and β-actin (housekeeping internal control). All antibodies were purchased from Abcam and diluted according to the manufacturer's instructions. An enhanced chemiluminescence (ECL) detection system (Amersham Biosciences) was used to visualize the immunoreactive bands. The relative protein levels were semi-quantified by densitometric analysis using Image J software.

7. Statistical analysis

Proper statistical tests to analyze the collected data were utilized via SPSS software (version 22). One-way analysis of variance (ANOVA) was applied to examine the differences among groups when analyzing data of body weight changes, normalized protein expression, proliferation, apoptosis, cellular, and microvessel density values followed by Tukey post hoc test was performed for pairwise comparisons. The probability of survival in tumor-bearing mice was estimated by Kaplan–Meier method, then log-rank test was done for inter-group comparisons. Two-

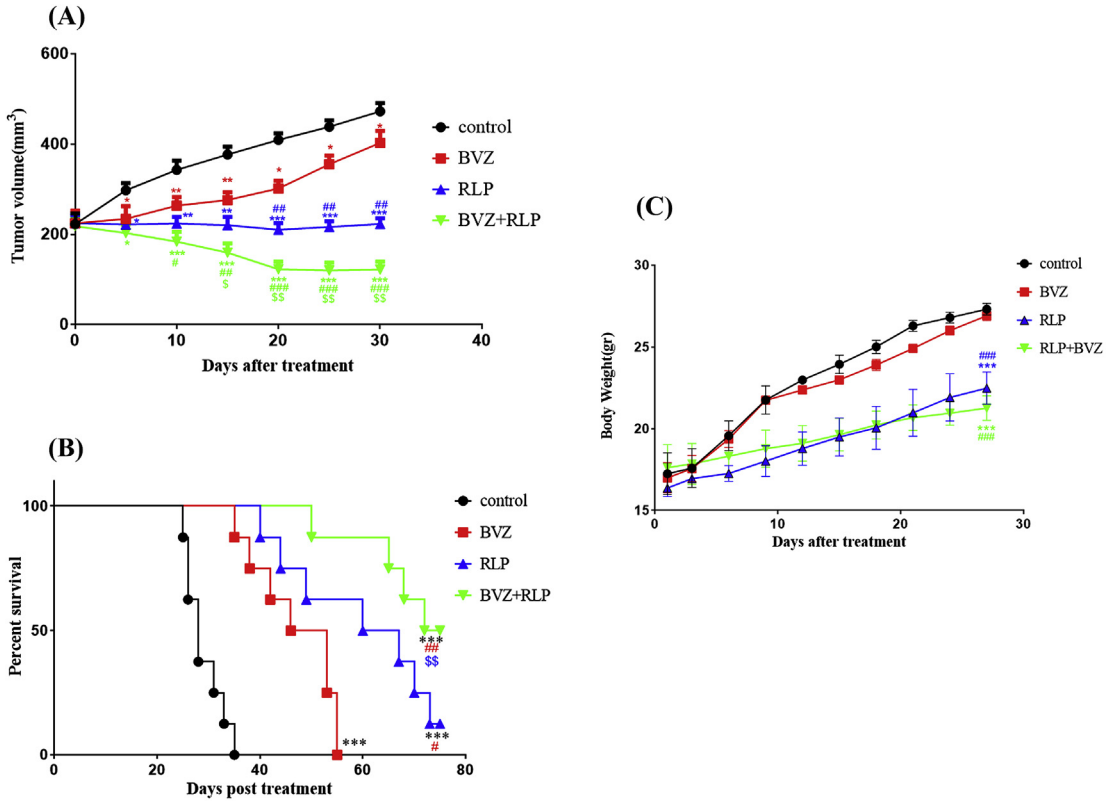

Fig. 1. Differences between various groups in terms of C6 tumor size at indicated time points (**A**), survival time of tumor-bearing mice (**B**) and body weight alteration during the time (**C**) are illustrated. (**A**) Changes of mean tumor volume in all groups during the therapeutic course. For all treatment groups until the end of treatment ($n = 11$). For control group up to 20th day of treatment (n = 11); on 25th day and 30th of treatment, sample sizes were 10 and 6 mice, respectively. The descending curves depict a downward trend of tumor volume over time in rolipram and co-treatment groups (**B**). The survival percentage during the study (on 75th day after treatment onset) is plotted using Kaplan-Meier survival method. (**C**) The graph delineates body weight for each group during the treatment period. Data are expressed as mean ± SEM. $^{*}P < 0.05$, $^{**}P < 0.01$, $^{***}P < 0.001$ compared to the respective control; $^{\$}P < 0.05$, $^{\$\$}P < 0.01$ compared to the rolipram group; $^{\#}P < 0.05$, $^{\#\#}P < 0.01$, $^{\#\#\#}P < 0.001$ in comparison to bevacizumab alone. BVZ: Bevacizumab; RLP: Rolipram.

way mixed model ANOVA was used to examine the differences of tumor size between various groups during the time. We also applied one-way ANOVA and post hoc Tukey test to compare between groups in terms of tumor sizes at each fixed time point. All data were presented as mean ± standard error of mean (S.E.M). $P < 0.05$, $P < 0.01$ and $P < 0.001$ were considered as significance levels.

8. Results

8.1. Co-treatment with bevacizumab and rolipram strengthens the tumor growth inhibition induced by monotherapies in C6 xenografts-bearing mice

Based on the results depicted in Fig. 1A, the tumor volume was substantially enlarged by 2.1-fold at the final day of treatment compared to the tumor size at the initial day of a therapeutic course in the control group. Tumor growth from the beginning to approximately half a period of treatment was decelerated by bevacizumab. After that, there was a sudden acceleration. Both rolipram (11%) and co-treatment (45%) had a stable suppressive effect on the tumor growth during the dosing period. According to the results of two-way mixed model ANOVA, there was a significant interaction effect between time and group ($P < 0.001$). All treatment induced a time-dependent tumor growth inhibition versus control. According to one-way ANOVA results, the treatment-induced meaningful differences in tumor size relative to control was rapidly observed from fifth day after treatment onset to the end of a therapeutic period. However, the rate of tumor growth suppression in the combination therapy group was significantly more than that in single therapies. Pairwise comparisons indicated that a more tumor shrinkage developed by rolipram compared to bevacizumab ($P < 0.01$). More details of intergroup comparisons at separated time points during the treatment period are displayed in Fig. 1A.

8.2. All treatments lengthen the survival of C6 tumor-bearing mice in parallel with a body weight gain over time

Fig. 1B displayed a longer median survival time about 73 (95% CI = 66–82) days in mice treated with the bevacizumab plus rolipram as compared to those treated with bevacizumab (49 days; 95% CI = 36–58, $P < 0.01$) or rolipram (63 days; 95% CI = 46–77, $P < 0.01$) or control (28 days; 95% CI = 25–38, $P < 0.001$). Overall, 12.5% and 50% of mice, in rolipram alone and combination therapy groups, respectively, survived by the end of the experiment. The results revealed a pronounced increase in lifespan of bevacizumab-treated mice (75%) relative to the control ($P < 0.001$). Likewise, rolipram group demonstrated a higher lifespan about 125% and 28.57% as compared to control ($P < 0.001$) and bevacizumab alone ($P < 0.05$), respectively. Combination therapy significantly prolonged the lifespan by 160.71%, 48.97%, and 15.87% in comparison with control, bevacizumab and rolipram alone, respectively. As shown in Fig. 1C, rolipram alone similar to co-treatment resulted in a predominant loss of body weight versus bevacizumab monotherapy and control ($P < 0.001$).

8.3. Combination therapy potentiates the cellular density reduction induced by monotherapies in C6 xenografts

All treatments represented a lower cellular density versus control consistent with the data based on the tumor growth inhibition obtained

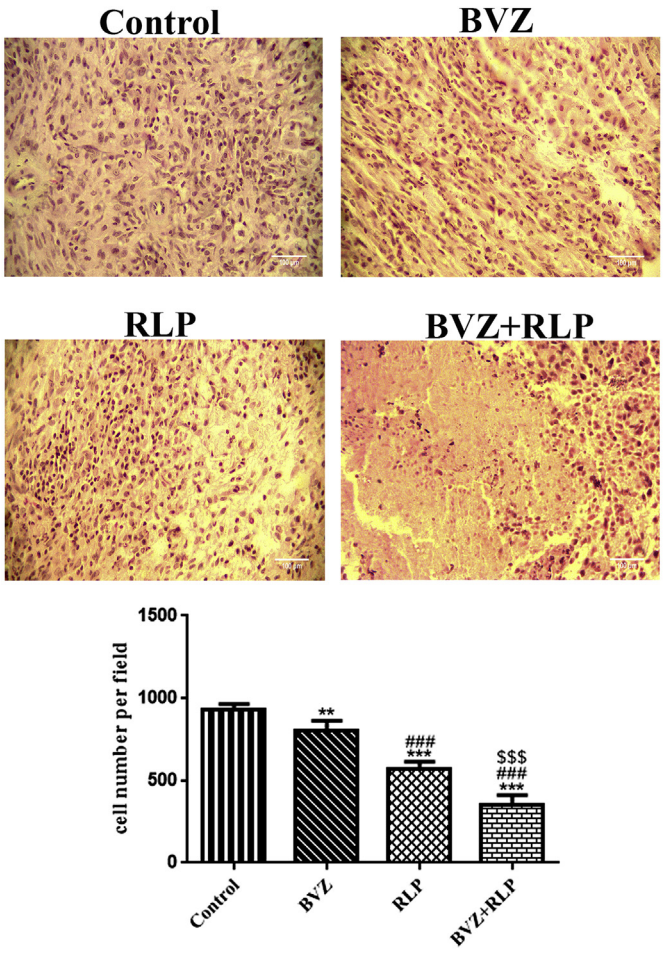

Fig. 2. Results of comparing the cellular density values in C6 glioma xenografts among various groups are illustrated. H&E staining was done to evaluate the cellular density. The images were captured at 200× magnification. The bars display the mean value of cellular density/field in xenografts from all groups (n = 3/group). An extensive cell-free zone is observed in tumor section relevant to co-treatment. Data are presented as mean ± SEM. $^{**}P < 0.01$, $^{***}P < 0.001$ compared to control; $^{###}P < 0.001$ compared to bevacizumab, $^{$$$}P < 0.001$ in comparison to rolipram. BVZ: Bevacizumab; RLP: Rolipram; H&E: Hematoxylin & Eosin.

in the present study. Apparently, combined treatment schedule yielded an outstanding reduction of cellular density in comparison with single therapies ($P < 0.001$). Cellular density in xenografts exposed to rolipram was dramatically less than that in bevacizumab-treated ones ($P < 0.001$). More details are illustrated in Fig. 2.

8.4. Single and combined therapies with rolipram reverse the bevacizumab-induced increment of the cell proliferation in C6 xenografts

The high values of Ki67-positive cells were observed in the tumor sections belonging to the control group. Unexpectedly, application of bevacizumab developed the more extensive areas containing Ki67-positive cells in relevant sections versus control ($P < 0.05$). Conversely, the mean normalized percentage of Ki67-positive cells was extremely lower in both co-treatment and rolipram-treated xenografts as compared with xenografts pertaining to control and bevacizumab ($P < 0.001$) groups. There were no significant differences between xenografts exposed to rolipram plus bevacizumab and those treated with rolipram alone in terms of cell proliferation ($P > 0.05$) (Fig. 3A).

8.5. All treatments markedly induce cell apoptosis in C6 xenografts

The results showed a distinguished induction of apoptosis by both single and combined therapeutic approaches as compared to control. Nevertheless, the proapoptotic effect of rolipram was significantly more than that of bevacizumab alone ($P < 0.05$). Co-administration of rolipram and bevacizumab intensively boosted the apoptosis rate in comparison with monotherapy protocols ($P < 0.001$). Fig. 3B depicts more data.

8.6. Concurrent application of rolipram and bevacizumab intensifies the antiangiogenesis activity exerted by each treatment alone

According to Fig. 4A, the mean percentage of CD31-positive cells similarly diminished in monotherapies-treated xenografts as compared to control ($P < 0.001$). It was also discovered that combined strategy caused an impressive antiangiogenesis effect versus control ($P < 0.001$), bevacizumab ($P < 0.05$) and rolipram ($P < 0.01$) alone. Likewise, on the basis of the Western blot results, a more relative quantity of CD31 protein expression was detected in co-treated tumor lysates compared to control ($P < 0.001$) and each treatment alone ($P < 0.01$). In the case of single therapies, the findings concerning the relative levels of CD31 expression corroborated the data related to CD31 immunohistochemistry. (Upper right panel in Fig. 4B).

8.7. The effect of treatments on relative expression of PDE4A, HIF1α, phospho-AKT, p53, CA9 and cleaved-caspase3 proteins in C6 xenografts

As shown in Fig. 4B, bevacizumab therapy conspicuously elevated the relative levels of PDE4A ($P < 0.01$), HIF1α, CA9, cleaved-caspase3 ($P < 0.001$) and phospho-AKT ($P < 0.05$) proteins in comparison with control. Also, there was a measurable decrease in mean normalized protein expression of p53 by bevacizumab ($P < 0.001$). Conversely, Rolipram and co-treated tumors showed a significant depletion of normalized protein density in the immunoreactive bands pertaining to the PDE4A, HIF1α, and phospho-AKT as well as an substantial increase in p53 levels in as compared to control and bevacizumab-treated ones ($P < 0.001$). There were subtle differences in relative levels PDE4A, HIF1α, and phospho-AKT ($P > 0.05$) but not p53 ($P < 0.001$) between rolipram and combined groups. Rolipram and co-treatment increased CA9 levels relative control ($P < 0.001$). Interestingly, upregulation of CA9 induced by co-treatment was significantly more than monotherapies ($P < 0.001$). Clearly, co-treatment considerably heightened the relative levels of cleaved-caspase3 expression in contrast to control, bevacizumab and rolipram ($P < 0.001$) alone. Nonetheless, rolipram-induced upregulation of cleaved-caspase3 was more than that developed by bevacizumab alone ($P < 0.01$).

9. Discussion

In spite of that bevacizumab is widely used in GBM therapy, it quickly begets only a temporary good response in patients [9] and ultimately it fails to control of the GBM after a few months of treatment initiation [29]. Today, optimal dose and timing of bevacizumab application is a controversial matter in the context of GBM treatment [30]. In this regards, we found that a low-dose administration of the bevacizumab for eleven times every two days once primarily slowed down the growth of tumor up to twenty day after the treatment onset; however, in a few final doses of the treatment from day 20–30, bevacizumab demonstrated an abrupt acceleration in the tumor development. These results were consistent with a decay in cellular and vascular density and an increase in cell proliferation, apoptosis, and relative expression of PDE4A, phospho-AKT, cleaved caspase3, CA9 and HIF1α proteins within relevant xenografts evaluated at the end of treatment. Despite a more intratumor cell proliferation in bevacizumab group relative to control, a sensible slow tumor growth might result from the

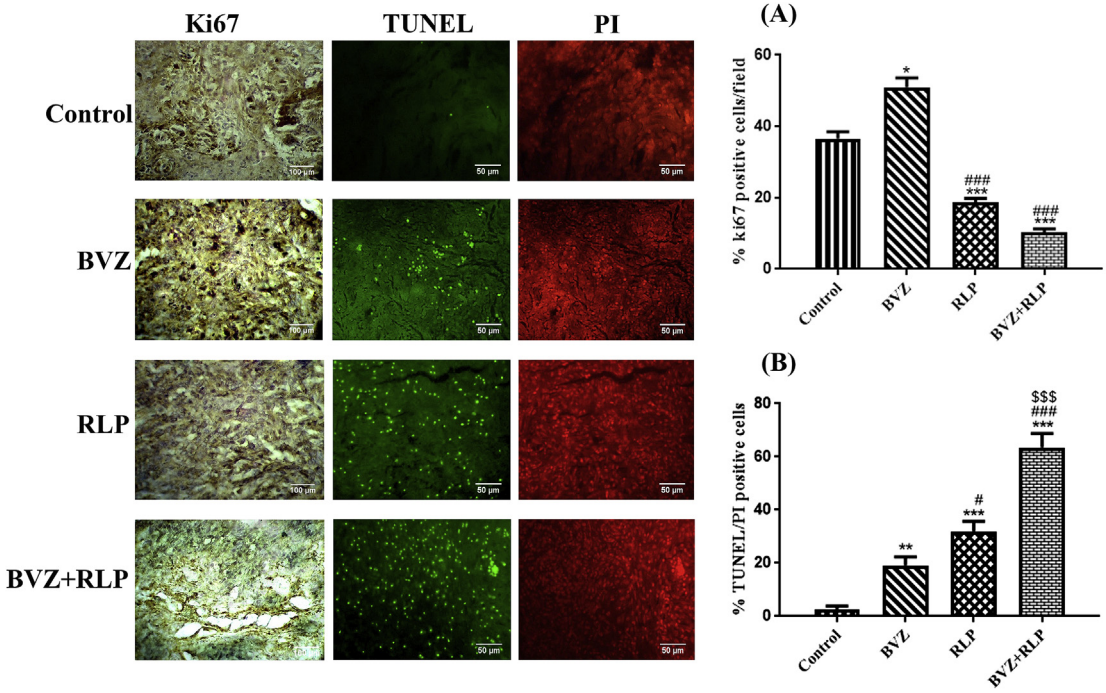

Fig. 3. Effects of treatment on the amount of cell proliferation (**A**) and apoptosis (**B**) in C6 glioma xenografts are shown. Ki67-stained proliferative cells (dark brown color) were visualized by immunohistochemistry technique under an inverted microscope (magnification = 200×). Green nuclei are apoptotic cells in representative fields of tumor sections pertaining to various treatment groups, and red nuclei are total cells of same fields (magnification = 400×). Image J was used to semi-quantify the cells. (**A**) The bars show the mean percentage of ki67-labeled nuclei/field in relevant xenografts of indicated groups (n = 3/group). (**B**) The bars show mean percentage of TUNEL positive cells normalized to the respective PI nuclei number in xenografts belonging to indicated groups (n = 3/group). The cell apoptosis within co-treated xenografts outranks. The data are presented as mean ± SEM. $^{*}P < 0.05$, $^{**}P < 0.01$, $^{***}P < 0.001$ compared to control; $^{\#}P < 0.05$, $^{\#\#\#}P < 0.001$ compared to the bevacizumab group; $^{\$\$\$}p < 0.001$ in comparison with rolipram alone. BVZ: Bevacizumab; RLP: Rolipram; TUNEL: Terminal deoxynucleotidyl transferase dUTP nick end labeling; PI: Propidium iodide. (For interpretation of the references to color in this figure legend, the reader is referred to the Web version of this article.)

antivascular and proapoptotic action of the drug, leading to a delay in animal death. As expected, present findings based on the antivascular and therapeutic effect of bevacizumab corroborated the results of our study [23] and others' ones [28,31] in the past. However, the current data concerning to the high rate of cell proliferation was contrary to our previous report that highlighted an insignificant cell proliferation reduction in C6 glioma xenografts exposed to bevacizumab for 12 days which was roughly equivalent to half the treatment period in this study [23]. Given the same interval time of sequential doses in both studies, this discrepancy may arise from a difference in the duration of therapeutic plan applied between two studies. It seems that the pro-proliferative action of bevacizumab may be triggered when the frequency of drug administration exceeds, probably giving rise to the unexpected acceleration of tumor growth at the last days of treatment.

However, single or combined therapies with rolipram generated a substantial tumor growth regression that started at approximately the beginning of treatment and constantly boosted until the therapies were terminated. Predictably, the mice which received both single and combined strategies of rolipram therapy demonstrated a longer survival and notable tumor shrinkage versus bevacizumab.

Furthermore, a durable favorable response to rolipram alone and co-treatment versus bevacizumab monotherapy might be due to a substantial antiproliferative effect of treatments using rolipram in contrast to pro-proliferative function of bevacizumab. Based on the current data, we found that bevacizumab-induced microvessel density reduction induced a relatively modest hypoxia detected by intratumor CA9 levels and caused the increase in HIF1α levels. On the basis of the positive regulatory action of HIF1α on the PDE4A expression already noted [19], it is suggested that long-term use of bevacizumab produces a hypoxia-dependent HIF1α upregulation, leading to the intratumor PDE4A overexpression. Functionally, PDE4 regulates intracellular levels of cyclic adenosine monophosphate (cAMP) [32] and takes part in tumorigenesis via the degradation of cAMP [25] which is involved in the cell fate [33] and AKT inhibition [34–37]. Physiologically, AKT is a key intracellular transducer of cell growth-promoting signals [38], and its inactivation participates in intrinsic proapoptotic pathway and caspase activities [39,40]. Mechanistically, it is guessed that high expression of PDE4A caused by bevacizumab brings about the AKT overactivation presumably through a depletion of intracellular c-AMP, leading to a great tumor cell proliferation and eventually a poor tumor growth suppression and shorter survival in bevacizumab group versus other treatments. Another explanation may be that an increase in HIF1α induction in bevacizumab-treated xenografts may cause an enhancement of hexokinase II mediated-aerobic glycolysis [6] stimulating the production of metabolites that may benefit proliferating cells [41]. Despite the equal effects of monotherapies and even a stronger action of co-treatment on the microvessel density reduction and hypoxia induction, it is thought that inhibiting PDE4 by rolipram alone and combined to bevacizumab might oppose the hypoxia-dependent HIF1α induction induced by vessel pruning due to treatments probably through a positive feedback loop of PDE4A and HIF1α, leading to the suppression AKT-dependent cell growth promoting signals and cell proliferation. Nevertheless, antiproliferative action of the co-treatment method was similar to rolipram alone, suggesting that co-treatment-induced antiproliferation did not play a part in its efficiency superiority versus rolipram alone.

However, it is not unlikely that the block of AKT-dependent proapoptotic signals by bevacizumab participates in less apoptosis induction, leading to a minimal repressive effect of this medical agent on the tumor progression relative to other treatments. We found that bevacizumab decreased intratumor p53 levels while rolipram monotherapy and co-treatment enhanced its levels. These changes appears to be

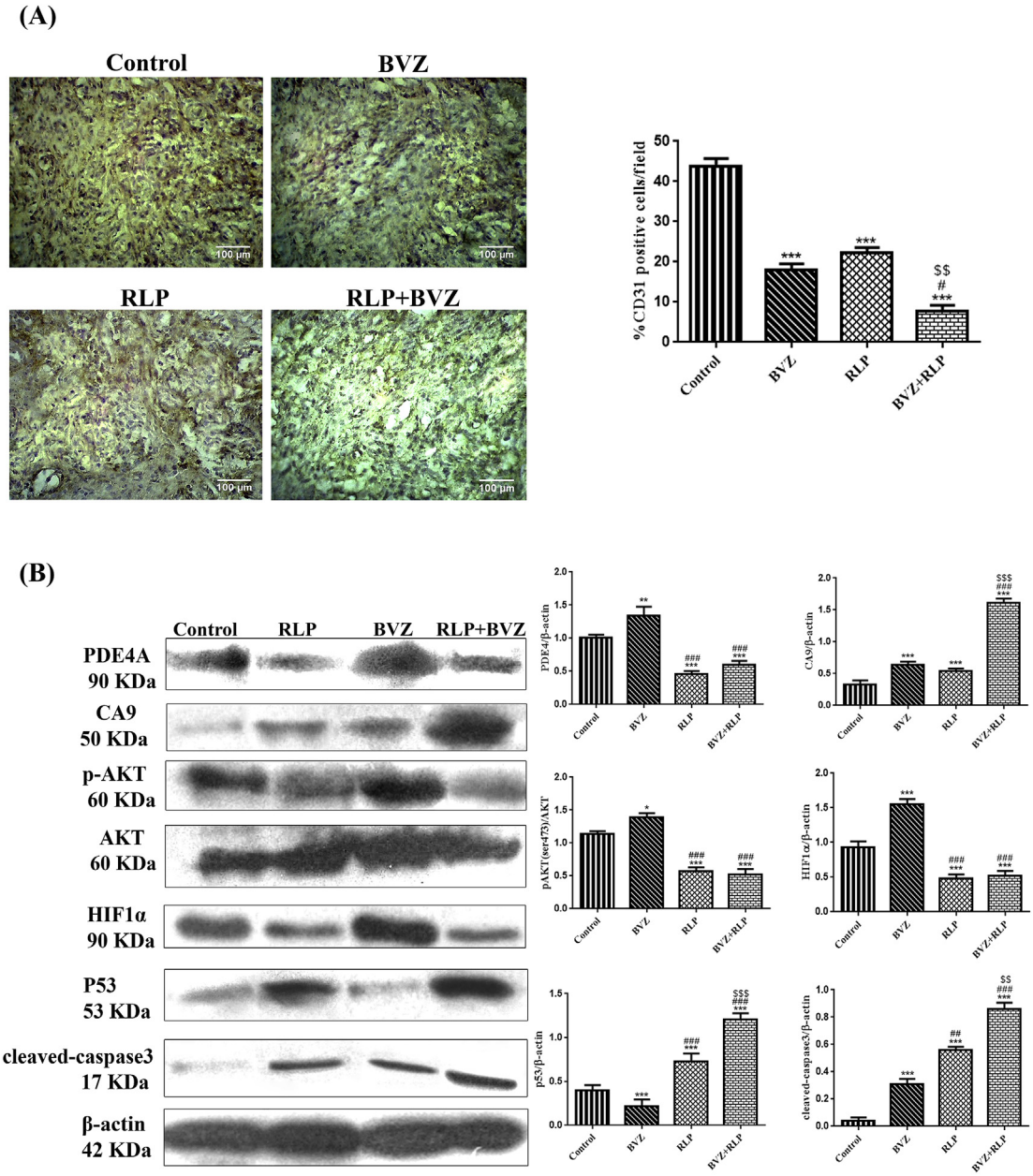

Fig. 4. Effects of treatment on the microvessel density (A) and expression of indicated proteins (B) in C6 xenografts are represented. (A) Immunohistochemistry was performed to detect the CD31-stained cells. The images illustrate CD31 positive cells (dark brown spots) in representative fields of tumor sections belonging to the indicated groups at magnification 200×. The bars show mean percentage of CD31 positive cells/field in xenografts from control mice and those receiving distinct treatments (n = 3/group). (B) Immunoreactive bands and relative expression of the indicated proteins in C6 glioma xenografts from control mice and those exposed to bevacizumab, rolipram or bevacizumab plus rolipram are displayed. The protein bands were provided using Western blot analysis and semi-quantified by densitometry technique using Image J software. Obtained results based on the target protein density pertaining to each treatment group were individually normalized to corresponding density of beta-actin. Data are presented as mean ± SEM (n = 3/group). $^{*}P < 0.05$, $^{**}P < 0.01$, $^{***}P < 0.001$ compared to control; $^{\#}P < 0.05$, $^{\#\#}P < 0.01$, $^{\#\#\#}P < 0.001$ as compared to bevacizumab group; and $^{\$\$}p < 0.01$, $^{\$}p < 0.05$ in comparison to rolipram group. BVZ: Bevacizumab; RLP: Rolipram; PDE4: phosphodiesterase IV; HIF1α: Hypoxia-inducible factor 1 α; Caspase3: Aspartate-specific cysteine protease 3. (For interpretation of the references to color in this figure legend, the reader is referred to the Web version of this article.)

associated with the alterations of HIF1α and phospho-AKT levels in the relevant xenografts. Particularly, p53 transcription factor is an essential tumor suppressor which involved in apoptosis process [42,43] and its transcriptional response and consequently p53-induced apoptosis process may be attenuated by HIF1α induction in a competitive manner [6]. Accordingly, it is suggested that bevacizumab-induced HIF1α up-regulation might weaken p53 stabilization. Besides, it is possible that bevacizumab induced-hyperactivation of AKT might trigger p53 degradation pathway by stimulating E3 ubiquitin ligase activity of murine double minute 2 (MDM2) [40]. However, it seems that active HIF1α and AKT related-pathways inhibiting p53 stabilization suppressed by rolipram, leading to more apoptosis induction versus bevacizumab. According to current data, proapoptotic signals stimulated by bevacizumab might be transmitted through the AKT-independent pathways triggering caspase3 activity. One of these pathways engaged in caspase3-dependent extrinsic apoptosis process is originated from tumor necrosis factor (TNF)-related apoptosis-inducing ligand (TRAIL) [42] that has been suggested its serum levels enhancement in response to bevacizumab [44]. Importantly, an additive apoptotic induction by co-treatment appears to be associated with a better therapeutic outcome

relative to monotherapies and may be mediated by a drastic caspase3 activation and p53 stabilization. A scenario for the explanation of more apoptosis induction in co-treated xenografts may be related to the severe hypoxia induction that is optimal condition for the stabilization of p53 [45]. Moreover, it is conceivable that the distinct caspase3-dependent proapoptotic pathways triggered by each treatment alone might be unified together, leading to the excellent proapoptotic and tumor regression in the co-treatment group. We also argue that more cellular density loss in co-treated tumors might be derived from a more apoptosis induction as compared to monotherapies.

Unexpectedly, our study highlighted a bevacizumab-like antivascular property of rolipram that was associated with the downregulation of intratumor PDE4A, phospho-AKT, HIF1α levels. In contrast, bevacizumab increased the expression of all the mentioned proteins. This denotes that antiangiogenesis effect of bevacizumab might be functionally independent of PDE4A, HIF1α and AKT signals. Herein, it seems that bevacizumab and rolipram alone impose an antivascular action through the individual pathways. Accordingly, it is guessed that the PDE4 inhibition by rolipram may suppress HIF1α-dependent angiogenesis pathways and leads to a decline in tumor neovascularization, as expected. In particular, co-treatment probably intensifies the antiangiogenesis effects of monotherapies through the integration of individual antivascular pathways triggered by each therapeutic agent alone. Additionally, it is possible that the bevacizumab-induced vascular normalization [28,46–48] and optimal drug delivery [49,50] maximizes the tumoral cytotoxicity and clinical improvement. In the end, it is mentioned that rolipram at the clinical dose could be relatively tolerable [51]. Besides, it readily penetrates into the central nervous system [52], emphasizing its application for GBM therapy in medical practice.

10. Conclusion

Altogether, this study highlighted that a minor therapeutic effect of bevacizumab may be due to its pro-proliferative and mild proapoptotic actions that appear to be associated with hypoxia-mediated HIF1α induction and activation of PDE4A/AKT/HIF1α pathway inhibiting p53 stabilization. These functions of bevacizumab counteracted by co-treatment, leading to the major apoptosis induction and therapeutic efficacy that seems to be mediated by the paramount p53 and caspase3 activities. We suggest that a similar study is required to do in the future on the orthotropic GBM models as well as FDA approved subfamily specific PDE4 inhibitors like roflumilast causing less systemic toxicity. Surely, the molecular characterization of bevacizumab-resistant tumors in terms of PDE4 levels for the identification of patients who may benefit from co-treatment is a critical priority to effectively exploit this new co-treatment in the clinic.

Funding

This project was funded by Guilan University of Medical Sciences (Grant No. 96100202).

Ethical approval

All applicable international, national, and/or institutional guidelines for the care and use of animals were followed. This article does not contain any studies with human participants performed by any of the authors.

Informed consent

For this type of study, formal consent is not required.

Declaration of competing interets

All authors declare that they have no conflict of interest.

Acknowledgments

The authors would like to thank the all staffs of Cellular and Molecular Research Center at Iran University of Medical Sciences and Cancer Research Center at Tehran University of Medical Sciences, who helped us in performing the animal care and treatment processes.

References

[1] D.S. Nørøxe, H.S. Poulsen, U. Lassen, Hallmarks of glioblastoma: a systematic review, ESMO open 1 (6) (2016) e000144.
[2] D.N. Louis, H. Ohgaki, O.D. Wiestler, W.K. Cavenee, P.C. Burger, A. Jouvet, B.W. Scheithauer, P. Kleihues, The 2007 WHO classification of tumours of the central nervous system, Acta Neuropathol. 114 (2) (2007) 97–109.
[3] E. Tastekin, V.Y. Caloglu, F. Puyan, B. Tokuc, M. Caloglu, T.D. Yalta, N. Can, B. Guler, Prognostic value of angiogenesis and survivin expression in patients with glioblastoma, Turk Neurosurg 26 (4) (2016) 484–490.
[4] M.E. Hardee, D. Zagzag, Mechanisms of glioma-associated neovascularization, Am. J. Pathol. 181 (4) (2012) 1126–1141.
[5] X. Lv, J. Li, C. Zhang, T. Hu, S. Li, S. He, H. Yan, Y. Tan, M. Lei, M. Wen, The role of hypoxia-inducible factors in tumor angiogenesis and cell metabolism, Genes & Diseases 4 (1) (2017) 19–24.
[6] A. Sendoel, M.O. Hengartner, Apoptotic cell death under hypoxia, Physiology 29 (3) (2014) 168–176.
[7] M.H. Cohen, Y.L. Shen, P. Keegan, R. Pazdur, FDA drug approval summary: bevacizumab (Avastin®) as treatment of recurrent glioblastoma multiforme, The Oncologist 14 (11) (2009) 1131–1138.
[8] A. Narayana, P. Kelly, J. Golfinos, E. Parker, G. Johnson, E. Knopp, D. Zagzag, I. Fischer, S. Raza, P. Medabalmi, Antiangiogenic therapy using bevacizumab in recurrent high-grade glioma: impact on local control and patient survival, J. Neurosurg. 110 (1) (2009) 173–180.
[9] W.B. Pope, A. Lai, P. Nghiemphu, P. Mischel, T. Cloughesy, MRI in patients with high-grade gliomas treated with bevacizumab and chemotherapy, Neurology 66 (8) (2006) 1258–1260.
[10] J.J. Vredenburgh, A. Desjardins, J.E. Herndon, J.M. Dowell, D.A. Reardon, J.A. Quinn, J.N. Rich, S. Sathornsumetee, S. Gururangan, M. Wagner, Phase II trial of bevacizumab and irinotecan in recurrent malignant glioma, Clin. Cancer Res. 13 (4) (2007) 1253–1259.
[11] J.F. de Groot, G. Fuller, A.J. Kumar, Y. Piao, K. Eterovic, Y. Ji, C.A. Conrad, Tumor invasion after treatment of glioblastoma with bevacizumab: radiographic and pathologic correlation in humans and mice, Neuro Oncol. 12 (3) (2010) 233–242.
[12] F. Iwamoto, L. Abrey, K. Beal, P. Gutin, M. Rosenblum, V. Reuter, L. DeAngelis, A. Lassman, Patterns of relapse and prognosis after bevacizumab failure in recurrent glioblastoma, Neurology 73 (15) (2009) 1200–1206.
[13] K.V. Lu, J.P. Chang, C.A. Parachoniak, M.M. Pandika, M.K. Aghi, D. Meyronet, N. Isachenko, S.D. Fouse, J.J. Phillips, D.A. Cheresh, VEGF inhibits tumor cell invasion and mesenchymal transition through a MET/VEGFR2 complex, Cancer Cell 22 (1) (2012) 21–35.
[14] T. Simon, B. Coquerel, A. Petit, Y. Kassim, E. Demange, D. Le Cerf, V. Perrot, J.-P. Vannier, Direct effect of bevacizumab on glioblastoma cell lines in vitro, NeuroMolecular Med. 16 (4) (2014) 752–771.
[15] J. Hartwich, W.S. Orr, C.Y. Ng, Y. Spence, C. Morton, A.M. Davidoff, HIF-1α activation mediates resistance to anti-angiogenic therapy in neuroblastoma xenografts, J. Pediatr. Surg. 48 (1) (2013) 39–46.
[16] S. Ma, S. Pradeep, W. Hu, D. Zhang, R. Coleman, A. Sood, The role of tumor microenvironment in resistance to anti-angiogenic therapy, F1000Research 7 (2018).
[17] G.N. Masoud, W. Li, HIF-1α pathway: role, regulation and intervention for cancer therapy, Acta Pharm. Sin. B 5 (5) (2015) 378–389.
[18] S. Mahase, R.N. Rattenni, P. Wesseling, W. Leenders, C. Baldotto, R. Jain, D. Zagzag, Hypoxia-mediated mechanisms associated with antiangiogenic treatment resistance in glioblastomas, Am. J. Pathol. 187 (5) (2017) 940–953.
[19] S. Pullamsetti, G. Banat, A. Schmall, M. Szibor, D. Pomagruk, J. Hδnze, E. Kolosionek, J. Wilhelm, T. Braun, F. Grimminger, Phosphodiesterase-4 promotes proliferation and angiogenesis of lung cancer by crosstalk with HIF, Oncogene 32 (9) (2013) 1121.
[20] A.N. Suhasini, L. Wang, K.N. Holder, A.-P. Lin, H. Bhatnagar, S.-W. Kim, A.W. Moritz, R.C. Aguiar, A phosphodiesterase 4B-dependent interplay between tumor cells and the microenvironment regulates angiogenesis in B-cell lymphoma, Leukemia 30 (3) (2016) 617.
[21] R. Sengupta, T. Sun, N.M. Warrington, J.B. Rubin, Treating brain tumors with PDE4 inhibitors, Trends Pharmacol. Sci. 32 (6) (2011) 337–344.
[22] S. Ramezani, N. Vousooghi, F.R. Kapourchali, M. Hadjighasem, P. Hayat, N. Amini, M.T. Joghataei, Rolipram potentiates bevacizumab-induced cell death in human glioblastoma stem-like cells, Life Sci. 173 (2017) 11–19.
[23] S. Ramezani, N. Vousooghi, F.R. Kapourchali, M.T. Joghataei, Perifosine enhances bevacizumab-induced apoptosis and therapeutic efficacy by targeting PI3K/AKT pathway in a glioblastoma heterotopic model, Apoptosis 22 (8) (2017) 1025–1034.
[24] T.C. Chen, P. Wadsten, S. Su, N. Rawlinson, F.M. Hofman, C.K. Hill, A.H. Schonthal,

The type IV phosphodiesterase inhibitor rolipram induces expression inhibitors p21Cip1 and p27Kip1, resulting in growth inhibition, increased differentiation, and subsequent apoptosis of malignant A-172 glioma cells, Cancer Biol. Ther. 1 (3) (2002) 268–276.
[25] P. Goldhoff, N.M. Warrington, D.D. Limbrick, A. Hope, B.M. Woerner, E. Jackson, A. Perry, D. Piwnica-Worms, J.B. Rubin, Targeted inhibition of cyclic AMP phosphodiesterase-4 promotes brain tumor regression, Clin. Cancer Res. 14 (23) (2008) 7717–7725.
[26] E.-Y. Moon, G.-H. Lee, M.-S. Lee, H.-M. Kim, J.-W. Lee, Phosphodiesterase inhibitors control A172 human glioblastoma cell death through cAMP-mediated activation of protein kinase A and Epac1/Rap1 pathways, Life Sci. 90 (9–10) (2012) 373–380.
[27] S. Ramezani, M. Hadjighassem, N. Vousooghi, M. Parvaresh, F. Arbabi, N. Amini, M.T. Joghataei, The role of protein kinase B signaling pathway in anti-cancer effect of rolipram on glioblastoma multiforme: an in vitro study, Basic Clin. Neurosci. 8 (4) (2017) 325.
[28] L.D. von Baumgarten, D. Brucker, A.L. Tirniceru, Y. Kienast, S. Grau, S. Burgold, J. Herms, F. Winkler, Bevacizumab has differential and dose-dependent effects on glioma blood vessels and tumor cells, Clinical Cancer Research:clincanres. 1868 (2011) 2010.
[29] M. Salas, M. Guzman, M. Judy, Bevacizumab: a controversial agent against high-grade gliomas, JHN J. 6 (2) (2011) 3.
[30] R. Stupp, M. Weller, Questions Regarding the Optimal Use of Bevacizumab in Glioblastoma: a Moving Target, Oxford University Press, 2014.
[31] A. Rapisarda, M. Hollingshead, B. Uranchimeg, C.A. Bonomi, S.D. Borgel, J.P. Carter, B. Gehrs, M. Raffeld, R.J. Kinders, R. Parchment, Increased antitumor activity of bevacizumab in combination with hypoxia inducible factor-1 inhibition, Mol. Cancer Ther. (2009) 1535–7163 MCT-1509-0274.
[32] M.D. Houslay, D.R. Adams, PDE4 cAMP phosphodiesterases: modular enzymes that orchestrate signalling cross-talk, desensitization and compartmentalization, Biochem. J. 370 (1) (2003) 1–18.
[33] P. Sassone-Corsi, The cyclic AMP pathway, Cold Spring Harbor perspectives in biology 4 (12) (2012) a011148.
[34] K. Hong, L. Lou, S. Gupta, F. Ribeiro-Neto, D.L. Altschuler, A novel Epac-Rap-PP2A signaling module controls cAMP-dependent Akt regulation, J. Biol. Chem. 283 (34) (2008) 23129–23138.
[35] S. Kim, K. Jee, D. Kim, H. Koh, J. Chung, Cyclic AMP inhibits Akt activity by blocking the membrane localization of PDK1, J. Biol. Chem. 276 (16) (2001) 12864–12870.
[36] P.G. Smith, F. Wang, K.N. Wilkinson, K.J. Savage, U. Klein, D.S. Neuberg, G. Bollag, M.A. Shipp, R.C. Aguiar, Blood 105 (1) (2005) 308–316.
[37] L. Wang, F. Liu, M.L. Adamo, Cyclic AMP inhibits extracellular signal-regulated kinase and phosphatidylinositol 3-kinase/Akt pathways by inhibiting Rap1, J. Biol. Chem. 276 (40) (2001) 37242–37249.
[38] B.D. Manning, A. Toker, AKT/PKB signaling: navigating the network, Cell 169 (3) (2017) 381–405.
[39] E. Fayard, L.A. Tintignac, A. Baudry, B.A. Hemmings, Protein kinase B/Akt at a glance, J. Cell Sci. 118 (24) (2005) 5675–5678.
[40] M. Grzmil, B.A. Hemmings, Deregulated signalling networks in human brain tumours, Biochim. Biophys. Acta Protein Proteonomics 1804 (3) (2010) 476–483.
[41] M.G. Vander Heiden, L.C. Cantley, C.B. Thompson, Understanding the Warburg effect: the metabolic requirements of cell proliferation, Science 324 (5930) (2009) 1029–1033.
[42] S. Fulda, K.-M. Debatin, Extrinsic versus intrinsic apoptosis pathways in anticancer chemotherapy, Oncogene 25 (34) (2006) 4798.
[43] S. Haupt, M. Berger, Z. Goldberg, Y. Haupt, Apoptosis-the p53 network, J. Cell Sci. 116 (20) (2003) 4077–4085.
[44] A. Bisgin, A. Kargi, A.D. Yalcin, C. Aydin, D. Ekinci, B. Savas, S. Sanlioglu, Increased serum sTRAIL levels were correlated with survival in bevacizumab-treated metastatic colon cancer, BMC Canc. 12 (1) (2012) 58.
[45] H. Suzuki, A. Tomida, T. Tsuruo, Dephosphorylated hypoxia-inducible factor 1α as a mediator of p53-dependent apoptosis during hypoxia, Oncogene 20 (41) (2001) 5779.
[46] L. Claesson-Welsh, M. Welsh, VEGFA and tumour angiogenesis, J. Intern. Med. 273 (2) (2013) 114–127.
[47] D. Fukumura, R.K. Jain, Tumor microvasculature and microenvironment: targets for anti-angiogenesis and normalization, Microvasc. Res. 74 (2–3) (2007) 72–84.
[48] R.K. Jain, Normalization of tumor vasculature: an emerging concept in anti-angiogenic therapy, Science 307 (5706) (2005) 58–62.
[49] S. Azzi, J.K. Hebda, J. Gavard, Vascular permeability and drug delivery in cancers, Frontiers in oncology 3 (2013) 211.
[50] P.V. Dickson, J.B. Hamner, T.L. Sims, C.H. Fraga, C.Y. Ng, S. Rajasekeran, N.L. Hagedorn, M.B. McCarville, C.F. Stewart, A.M. Davidoff, Bevacizumab-induced transient remodeling of the vasculature in neuroblastoma xenografts results in improved delivery and efficacy of systemically administered chemotherapy, Clin. Cancer Res. 13 (13) (2007) 3942–3950.
[51] E. Zeller, H.-J. Stief, B. Pflug, M. Sastre-y-Hernandez, Results of a phase II study of the antidepressant effect of rolipram, Pharmacopsychiatry 17 (06) (1984) 188–190.
[52] W. Krause, G. Kühne, Pharmacokinetics of rolipram in the rhesus and cynomolgus monkeys, the rat and the rabbit. Studies on species differences, Xenobiotica 18 (5) (1988) 561–571.